EARTHQUAKE ENGINEERING AND STRUCTURAL DYNAMICS
Earthquake Engng Struct. Dyn. 2000; **29**:683–691

Seismically induced racking of tunnel linings

Joseph Penzien*

International Civil Engineering Consultants, Inc., Berkeley, CA 94704, U.S.A.

SUMMARY

An analytical procedure is presented for evaluating the racking deformation of rectangular and circular tunnel linings caused by soil–structure interaction during a seismic event. The procedure, as applied to rectangular linings, is supplementary to that previously published by Penzien and Wu (*Earthquake Engineering and Structural Dynamics*, 1998; **27**:283–300) for circular linings. Copyright © 2000 John Wiley & Sons, Ltd.

KEY WORDS: tunnel linings; soil/lining interaction

INTRODUCTION

The most critical deformation produced in a tunnel lining during a seismic event is racking of the cross-section. Numerous authors have treated this subject, including Hoeg [1] in 1968, Peck *et al.* [2] in 1972, Owen and Scholl [3] in 1981, Merrit *et al.* [4] in 1985, and Wang [5] in 1993. Because the dimensions of a typical lining cross-section are small compared with the wavelengths in the dominant ground motions producing the racking, the lining cross-section can be assumed to be interacting with soil having a uniform strain field. Further, because inertia effects in both the lining and its surrounding soil as produced by soil–structure interaction are relatively small, the seismically induced racking deformations in a lining take place in essentially a quasi-static fashion. These two conditions form the basis of the procedure presented herein for evaluating the racking deformation of rectangular and circular tunnel linings.

RACKING OF RECTANGULAR LININGS

Consider a homogeneous isotropic soil medium subjected to a seismically induced uniform shear–strain field of intensity γ_{ff} as indicated in Figure 1(a). If an infinitely long rectangular cavity

* Correspondence to: Joseph Penzien, International Civil Engineering Consultants, Inc., 1995 University Avenue, Suite 119, Berkeley, CA 94704, U.S.A.

Received 13 July 1999
Revised 2 November 1999
Accepted 11 November 1999

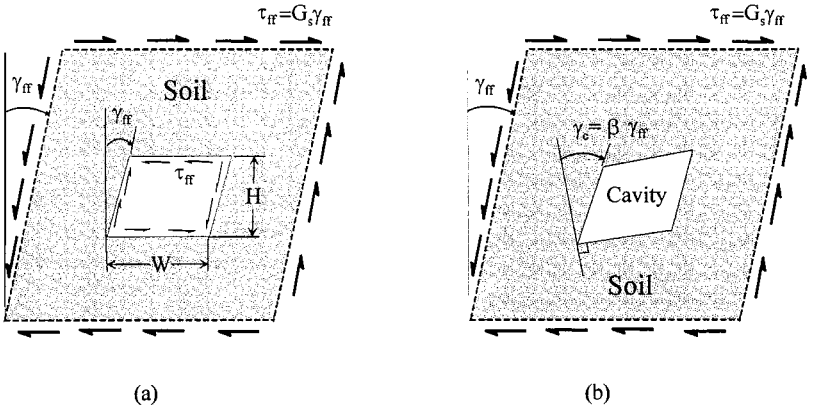

Figure 1. Deformation of rectangular cavity subjected to a uniform shear–strain environment: (a) with free-field shear stress distribution applied to cavity surface; (b) with free-field shear stress distribution removed from cavity surface.

having cross-section dimensions W and H is present in the original unstrained medium, it will experience the same free-field racking γ_{ff} provided the free-field shear stress τ_{ff} equal to $G_s\gamma_{ff}$ is applied as an external loading to the cavity surface. In this case, G_s is the strain-compatible shear modulus of the soil.

If the cavity surface loading τ_{ff} is removed, the cavity will further elongate along one diagonal and shorten along the other, increasing the cavity-racking angle from γ_{ff} to γ_c as indicated in Figure 1(b). Considering the racking to take place under the two-dimensional plane-strain condition, the racking ratio γ_c/γ_{ff}, denoted herein as β, can be obtained using the approximate relation

$$\beta \doteq 4(1 - v_s) \tag{1}$$

in which v_s is Poisson's ratio of the soil medium.

As shown in Reference [6], Equation (1) gives the exact value of racking ratio for a cylindrical cavity. In this case, racking is measured in terms of the cavity's diameter changes in the $\pm 45^\circ$ directions from the cross-section's horizontal axis. The free-field soil-compatible diameter changes, $\pm\Delta_{ff}$, in these directions equal $\pm\gamma_{ff}D/2$ in which D is the initial cavity diameter; and, the corresponding total diameter changes, $\pm\Delta_c$, after removing the free-field stresses from the cavity surface, equal $\pm\beta\Delta_{ff}$. The racking deformation in this cylindrical case takes place in an ovalling (or elliptical) mode with its principal axes in the $\pm 45^\circ$ directions.

To evaluate interaction of a rectangular tunnel lining with the free-field soil when strained to the level γ_{ff} as shown in Figure 1, use will be made of a soil stiffness coefficient k_{so} and a lining stiffness coefficient k_ℓ. The soil coefficient k_{so} is defined as that intensity of shear stress τ_{so} shown in Figure 2 which will produce a unit racking displacement of the soil outside the cavity as indicated under the plane-strain condition. Stiffness coefficient k_ℓ is defined as that intensity of shear stress τ_ℓ shown in Figure 3 which will produce the corresponding unit racking displacement of the lining under the plane-strain condition.

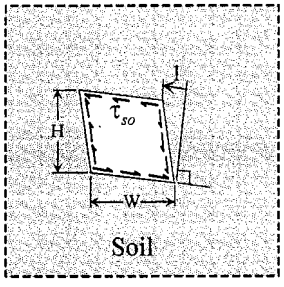

Figure 2. Stiffness coefficient $k_{so} = \tau_{so}$ for soil outside of cavity.

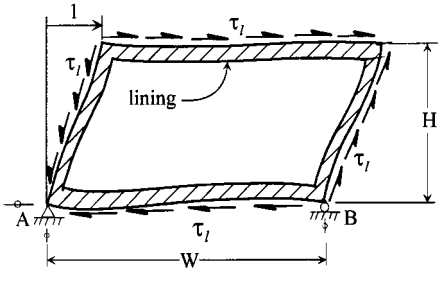

Figure 3. Stiffness coefficient $k_l \equiv \tau_l$ for rectangular lining.

Stiffness coefficient k_{so} is easily obtained since release of the *in situ* stress distribution τ_{ff} from the cavity wall produces a racking angle change equal to $\gamma_c - \gamma_{ff}$; thus, the stiffness k_{so} is given by

$$k_{so} = \tau_{ff}/(\gamma_c - \gamma_{ff})H \tag{2}$$

Since τ_{ff} equals $G_s\gamma_{ff}$ and γ_c equals $\beta\gamma_{ff}$, in which β is given by Equation (1), Equation (2) can be expressed in the form

$$k_{so} = G_s/(3 - 4\nu_s)H \tag{3}$$

The stiffness coefficient k_ℓ can be obtained through a simple static analysis of the lining subjected to the shear loading shown in Figure 3 under the plane-strain condition. Note that the shear loading of the lining in this figure is in self-equilibrium, thus resulting in zero reaction forces at support points A and B. While the arbitrary support conditions shown at these points can be assumed for the static solution in finding k_ℓ, the lining will, in addition to the racking indicated, actually rotate somewhat counterclockwise as a rigid body as it interacts with the free-field soil environment.

To evaluate soil–lining interaction, the approximate compatibility equation

$$\Delta_{i\ell} + \Delta_{is} \doteq 4(1 - \nu_s)\gamma_{ff}H \tag{4}$$

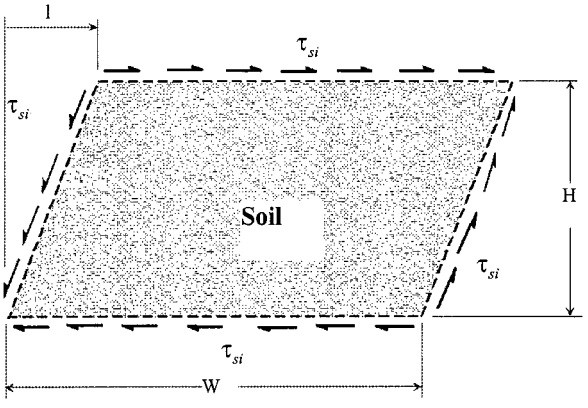

Figure 4. Stiffness coefficient $k_{si} \equiv \tau_{si}$ for rectangular lining.

is used in which $\Delta_{i\ell}$ is the lining racking displacement produced by its interaction with the soil and Δ_{is} is the decrease in soil cavity racking displacement produced by its interaction with the lining. Also, the approximate equilibrium equation

$$k_{so}\Delta_{is} \doteq k_{\ell}\Delta_{i\ell} \tag{5}$$

is used. Equations (4) and (5) have presented as being approximate relations because the normal stresses which develop at the interface of the lining and soil during interaction have been ignored. These normal stresses have a secondary effect on racking of the lining in this case however; thus, justifying use of the approximate relations given by Equations (4) and (5).

A second soil coefficient k_{si} is now defined as that intensity of shear stress τ_{si} acting on the outside of the soil of cross-section dimensions $W \times H$ in Figure 4 which will produce the unit racking displacement indicated. Because of the uniform shear strain within this body of soil, racking stiffness k_{si} is given by the relation

$$k_{si} = G_s/H \tag{6}$$

Comparing Equations (3) and (6), one observes that

$$k_{so} = k_{si}/(3 - 4\nu_s) \tag{7}$$

A lining–soil racking ratio R defined as $\Delta_{i\ell}/\Delta_{ff}$ is now obtained by substituting the free-field soil racking displacement Δ_{ff} which equals $\gamma_{ff}H$ into Equation (4) and Equation (7) into Equation (5) and then solving the resulting two equations for $\Delta_{i\ell}/\Delta_{ff}$ giving

$$R = \left[\frac{4(1 - \nu_s)}{1 + \alpha_s}\right] \tag{8}$$

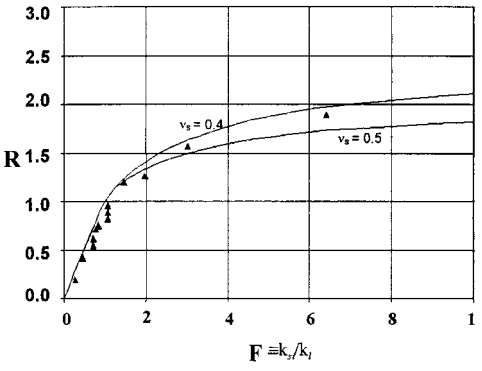

Figure 5. Racking ratio R verses stiffness ratio k_{si}/k_l for discrete values of Poisson's ratio v_s.

in which

$$\alpha_s = (3 - 4v_s)\frac{k_\ell}{k_{si}} \tag{9}$$

Equation (8) has been plotted as a function of the stiffness ratio k_{si}/k_ℓ in Figure 5 for discrete values of v_s equal to 0.4 and 0.5. This stiffness ratio has been defined as a flexibility coefficient F by the previous authors referenced [1–4]. The triangular points in this figure correspond to the published results of Wang [5], each of which was obtained through a separate finite-element dynamic solution. The soil Poisson's ratios associated with these points fall in the range $0.40 \leqslant v_s \leqslant 0.48$. The close agreement between the points in Figure 5 and the curves plotted for Equation (8) confirms the earlier statement that inertia effects in the lining and surrounding soil as caused by soil–structure interaction are relatively small; thus, they may be ignored in evaluating the racking of tunnel linings. Also, this close agreement confirms the earlier statement that the normal stresses produced on the lining surface during its interaction with the soil have a secondary effect on racking of the lining.

RACKING OF CIRCULAR LININGS

While Equation (8) was developed above for treating rectangular tunnel linings, it is valid for use in evaluating the seismically induced racking of circular linings as well. In fact, it is an exact expression of the ratio of the principal diameter change, $\Delta_{i\ell}$, of a circular lining to the principal diameter change, Δ_{ff}, of an imaginary circle of the same initial diameter when both interact with the same uniformly strained, γ_{ff}, free-field soil environment. In this circular-lining case, Equation (8) can be used to evaluate the principal racking (diameter-change) ratios $R = \pm\,\Delta_{i\ell}/\Delta_{ff}$ produced in the $\pm 45^\circ$ directions from the cross-section horizontal axis. In doing so, the generalized lining stiffness k_ℓ and the generalized outside-soil stiffness k_{so} published in Reference [6] can be used. Stiffness k_ℓ is defined as that value of σ shown for the pure-shear loading in Figure 6 which will produce unit diameter changes of the lining in the principal directions

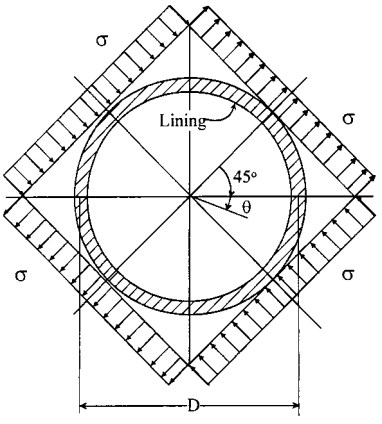

Figure 6. Stiffness coefficient $k_\ell \equiv \sigma_\ell$ for unit change in diameters along principal axes.

($\theta = \pm (\pi/4)$); and stiffness k_{so} is defined as that value of σ for the pure-shear loading shown in Figure 6 which, when applied in the opposite directions to the cylindrical cavity wall will produce unit cavity-wall diameter changes of opposite signs in the same principal directions, These stiffnesses as presented in Reference [6] are

$$k_\ell = \frac{48 E_\ell I_\ell}{D^4 (1 - \nu_\ell^2)} \tag{10}$$

$$k_{so} = \frac{2G_s}{D(3 - 4\nu_s)} \tag{11}$$

in which D is the outside diameter of the circular lining, and ν_ℓ, E_ℓ, and I_ℓ denote its Poisson's ratio, Young's modulus, and circumferential cross-section moment of inertia per unit of longitudinal dimension, respectively. The corresponding inside-soil generalized stiffness k_{si} can be obtained by substituting Equation (11) into Equation (7) giving

$$k_{si} = \frac{2G_s}{D} \tag{12}$$

The stiffness ratio k_ℓ / k_{si} now becomes

$$\frac{k_\ell}{k_{si}} = \frac{24 E_\ell I_\ell}{D^3 G_s (1 - \nu_\ell^2)} \tag{13}$$

Substituting Equation (13) into Equation (9) and the resulting expression for α_s into Equation (8) yields the principal racking ratios

$$R = \pm \frac{4(1 - \nu_s)}{(\alpha_s + 1)} \tag{14}$$

in which

$$\alpha_s \equiv \frac{k_\ell}{k_{so}} = \frac{24(3-4\nu_s)E_\ell I_\ell}{D^3 G_s(1-\nu_\ell^2)} \tag{15}$$

The principal lining–soil racking ratios represented by Equations (14) and (15) are fully consistent with the results presented in Reference [6], thus showing that Equation (8) can be used for the circular lining as well as for the rectangular lining. In the case involving the circular lining, both normal and shear stresses at the lining–soil interface are fully accounted for in deriving the expressions for stiffnesses k_ℓ and k_{so} given by Equations (10) and (11), respectively. In fact, the normal stresses are as important as the shear stresses in this case; thus, their effects must be included.

Having evaluated Δ_ℓ using $R\Delta_{ff}$, the corresponding circumferential internal force components in the circular lining per unit of longitudinal dimension can be determined as a function of angular position θ measured clockwise from the cross-section's horizontal axis using the relations

$$P(\theta) = -\frac{24E_\ell I_\ell \Delta_\ell}{D^3(1-\nu_\ell^2)}\cos 2\left(\theta + \frac{\pi}{4}\right) \tag{16}$$

$$M(\theta) = -\frac{6E_\ell I_\ell \Delta_\ell}{D^2(1-\nu_\ell^2)}\cos 2\left(\theta + \frac{\pi}{4}\right) \tag{17}$$

$$V(\theta) = -\frac{24E_\ell I_\ell \Delta_\ell}{D^3(1-\nu_\ell^2)}\sin 2\left(\theta + \frac{\pi}{4}\right) \tag{18}$$

in which $P(\theta)$, $M(\theta)$, and $V(\theta)$ are the axial force, moment, and shear components, respectively, which follow the sign conventions shown in Figure 7.

The above treatment of the circular lining assumes that no slippage occurs along the interface between soil and lining during the occurrence of a seismic event. Should it be decided that full slippage is likely to occur during a maximum design event, the above general procedure can still be used but with modified stiffness values as found in Reference [6], namely, the following:

$$k_\ell^n = \frac{72E_\ell I_\ell}{D^4(1-\nu_\ell^2)} \tag{19}$$

$$k_{so}^n = \frac{6G_s}{D(5-6\nu_s)} \tag{20}$$

in which the superscript 'n' has been added to indicate normal loading only, i.e., the tangential loading has been removed consistent with the assumption of full slippage.

Equation (14) is still valid in this full-slippage case, except that α_s should be replaced by α_s^n as expressed by

$$\alpha_s^n \equiv \frac{k_\ell^n}{k_{so}^n} = \frac{12E_\ell I_\ell(5-6\nu_s)}{D^3 G_s(1-\nu_\ell^2)} \tag{21}$$

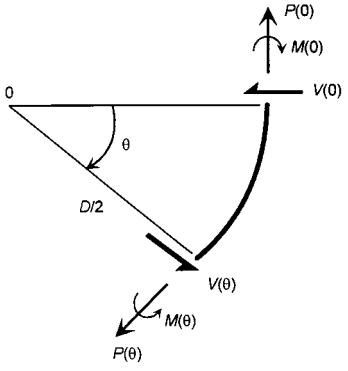

Figure 7. Sign convention for force components in circular lining.

Multiplying the resulting value of R, denoted as R^{n} to indicate full slippage, into the relation

$$\pm\Delta_{\ell}^{\mathrm{n}} = \pm\, R^{\mathrm{n}}\Delta_{\mathrm{ff}} \tag{22}$$

gives the principal diameter changes of the lining due to its interaction with the free-field soil. The corresponding internal axial force, moment, and shear in the lining can then be obtained using

$$P(\theta) = -\frac{12E_{\ell}I_{\ell}\Delta_{\ell}^{\mathrm{n}}}{D^3(1-\nu_{\ell}^2)}\cos 2\left(\theta+\frac{\pi}{4}\right) \tag{23}$$

$$M(\theta) = -\frac{6E_{\ell}I_{\ell}\Delta_{\ell}^{\mathrm{n}}}{D^2(1-\nu_{\ell}^2)}\cos 2\left(\theta+\frac{\pi}{4}\right) \tag{24}$$

$$V(\theta) = -\frac{24E_{\ell}I_{\ell}\Delta_{\ell}^{\mathrm{n}}}{D^3(1-\nu_{\ell}^2)}\sin 2\left(\theta+\frac{\pi}{4}\right) \tag{25}$$

FREE-FIELD SOIL ENVIRONMENT

To conduct the above racking analysis, it is assumed that the free-field soil response during an earthquake is in the transverse direction to the tunnel. From a standard site-response analysis, using the vertically propagating shear-wave model, the distribution of horizontal free-field ground displacement with depth y, namely $u(y, t)$, is obtained. In this analysis, one finds the critical distribution $u(y, t_{\mathrm{c}})$ at time t_{c} which produces the maximum shear-type deformation of the soil over depth D of the intended tunnel. The function $u(y, t_{\mathrm{c}})$ will usually be reasonably linear over this range so that γ_{ff} can be evaluated using the relation

$$\gamma_{\mathrm{ff}} = \frac{u(y_{\mathrm{t}}, t_{\mathrm{c}}) - u(y_{\mathrm{b}}, t_{\mathrm{c}})}{D} \tag{26}$$

in which y_t and y_b are the values of y at the top and bottom surface elevations of the intended tunnel lining, respectively.

CONCLUDING STATEMENT

The analysis procedure presented herein applies to tunnel linings having burial depths sufficiently large so that the free-surface boundary condition at the top of the soil has little effect on the racking soil–structure interaction. As shown by Wang in Reference [5], this boundary effect is negligible for rectangular linings when the ratio of the burial depth h (ground surface to mid-height of the lining) to the 'outside-to-outside' vertical dimension H of the lining, h/H, is greater than 1.5. As h/H reduces from this value, the racking ratio R will decrease rather slowly, even for a fixed value of γ_{ff}. This decrease is only about 20 per cent when h/H reduces from 1.5 to 0.5 showing the insensitivity of the racking ratio R to depth of burial. This same insensitivity of racking ratio with burial depth h also applies to circular linings. As shown by Penzien and Wu in Reference [6], the soil strains produced by soil-lining interaction are approximately proportional to $1/r^2$, r being radial distance from the center of the lining. Considering, for example, $r = 3R$, i.e., a distance of one diameter outside the lining, the soil strains will be only approximately 1/9 their values at the lining boundary. Thus, it is quite apparent that the effects of the free-surface boundary condition at the top of the soil can usually be neglected for typical burial depths.

The analytical procedure presented herein permits the evaluation of internal force components in a lining produced by racking during a seismic event. In checking a design, these components should be added to the corresponding components present in the lining prior to the event. These latter components can be evaluated for a circular lining using the 'stress-relaxation-following-installation' method given in Reference [6]. As pointed out in Reference [2], the assumption of full slippage is considered most appropriate in evaluating these initial force components. However, assuming that full slippage will take place during the seismic event may not be valid because of the short time involved. To be on the conservative side, it would seem prudent to assume no slippage in evaluating a linings seismic response.

REFERENCES

1. Hoeg K. Stresses against underground structural cylinders. *Journal of the Soil Mechanics and Foundation Division*, ASCE, 1968; **94**(SM4).
2. Peck RB, Hendron AJ, Jr. Mohraz B. State of the art of soft-ground tunneling. *Proceedings of the RETC* 1972; **1**: 259–285.
3. Owen GN, Scholl RE. Earthquake engineering of large underground structures. Federal Highway Administration, FHWA/RD-80/195, 1981.
4. Merritt JL, Monsees JE, Hendron AJ. Seismic design of underground structures. *Proceedings of the RETC*, 1985; **1**: 104–131.
5. Wang JN. Seismic design of tunnels. Parsons Brinckerhoff, Inc., Monograph 7, 1993.
6. Penzien J, Wu CL. Stresses in linings of bored tunnels. *Earthquake Engineering and Structural Dynamics* 1998; **27**: 283–300.

